HHS Public Access

Author manuscript

Immunity. Author manuscript; available in PMC 2017 May 17.

Published in final edited form as:

Immunity. 2016 May 17; 44(5): 1204–1214. doi:10.1016/j.immuni.2016.04.008.

Maternal-derived hepatitis B virus e antigen alters macrophage function in offspring to drive viral persistence after vertical transmission

Yongjun Tian[*], **Cheng-fu Kuo**[*], **Omid Akbari**, and **Jing-hsiung James Ou**

Department of Molecular Microbiology and Immunology, University of Southern California Keck School of Medicine, Los Angeles, California, USA

Summary

In contrast to horizontal transmission of hepatitis B virus (HBV) between adults, which often leads to self-limited acute infection, vertical transmission of HBV from mother to child often leads to chronic infection. However, the mechanisms linking vertical transmission with chronic infection are not known. We developed a mouse model to study the effect of maternal HBV infection on HBV persistence in offspring and found that HBV carried by the mother impaired $CD8^+$ T cell responses to HBV in her offspring, resulting in HBV persistence. This impairment of $CD8^+$ T cell responses was mediated by hepatic macrophages, which were predisposed by maternal HBV e antigen (HBeAg) to support HBV persistence by upregulation of inhibitory ligand PD-L1 and altered polarization upon restimulation with HBeAg. Depletion of hepatic macrophages led to $CD8^+$ T cell activation and HBV clearance in the offspring, raising the possibility of targeting macrophages to treat chronic HBV patients.

Graphical abstract

Correspondence to: J.-H. James Ou, 2011 Zonal Avenue, HMR-401, Los Angeles, CA 90033, USA. Phone: 323-442-1720; Fax: 323-442-1721; jamesou@hsc.usc.edu.

[*]These authors contributed equally to this work.

Author Contributions

Y.T. and C.F.K. designed and analyzed the data. O.A. provided advices on immunological studies and assisted with flow cytometry analysis. J.H.J.O. directed the studies. Y.T. and J.H.J.O. also wrote the manuscript.

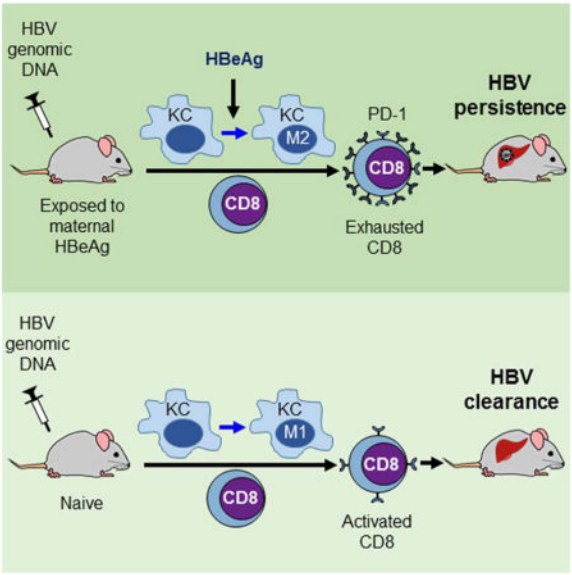

Keywords

Hepatitis B virus; HBV e antigen; Kupffer cells; PD-1; PD-L1; HBV vertical transmission

Introduction

Hepatitis B virus (HBV) infection in humans can cause severe liver diseases including cirrhosis and hepatocellular carcinoma. Globally, there are approximately 350 million people that are chronically infected by this virus, resulting in approximately 1 million deaths every year. Most chronic HBV carriers acquired the virus through vertical transmission from their infected mother early in life. In contrast to vertical transmission, horizontal transmission between adults usually leads to acute infection followed by viral clearance (Milich and Liang, 2003; Ou, 1997). Why vertical transmission frequently leads to HBV persistence whereas horizontal transmission does not is unclear. It has been suggested that this may be due to *in utero* tolerization of the fetal immune system to HBV antigens and/or the immaturity of the immune system of young children (Milich et al., 1990; Publicover et al., 2013; Publicover et al., 2011).

HBV is a hepatotropic virus and belongs to the hepadnavirus family. It has a small DNA genome of about 3.2 Kb. This genome contains four genes named S, X, P and C genes. The S gene codes for the viral envelope proteins known as surface antigens (HBsAg); the X gene codes for the regulatory protein HBx; the P gene codes for the viral DNA polymerase; and the C gene codes for the core protein, which forms the viral core particle, and a related protein named the precore protein, which is the precursor of the secreted e antigen (HBeAg) (Ou et al., 1986). The biological function of HBeAg is unclear. It is not essential for HBV replication, as mutations that abolish its expression do not negatively affect HBV replication in cell cultures (Lamberts et al., 1993), and HBV mutants incapable of expressing HBeAg have also been isolated from patients (Carman et al., 1989; Liu et al., 2004). However, based

on the observation that children born to women who carry the HBeAg-positive wild-type virus usually become chronic HBV carries without intervention whereas children born to women who carry HBeAg-negative HBV mutants usually develop self-limited acute HBV infection, it has long been suspected that HBeAg may be important for HBV to establish persistence after neonatal infection (Milich and Liang, 2003; Okada et al., 1976; Ou, 1997).

$CD8^+$ cytotoxic T lymphocyes (CTLs) play an important role in the clearance of HBV from patients (Chisari et al., 2010). However, in patients with chronic HBV infection, HBV-specific CTLs are frequently “exhausted”, which is a state of dysfunction defined by the progressive loss of key components of effector functions, resulting in the inability of patients to clear HBV infection (Maini and Schurich, 2010). Programmed death-1 (PD-1), an inhibitory member of the B7-CD28 family, is a major regulator for CTL exhaustion (Keir et al., 2008; Okazaki and Honjo, 2006). Upon binding to its ligand PD-L1 (also known as B7-H1), which is often expressed on antigen-presenting cells, PD-1 negatively regulates $CD8^+$ CTL responses and can suppress HBV-specific CTLs in the liver (Isogawa et al., 2013; Maier et al., 2007).

In this report, we developed a mouse model to study the mechanism of HBV persistence after vertical transmission. In this model, we used hydrodynamic injection to introduce a plasmid that contained the 1.3mer HBV genomic DNA into mouse hepatocytes. Although this DNA injection is not identical to natural HBV infection, once the HBV DNA enters mouse hepatocytes, it can direct HBV gene expression and replication (Tian et al., 2011; Yang et al., 2002). We found that HBV-negative mice born to HBV-positive mothers had impaired HBV-specific CTL response, leading to HBV persistence in these mice after the injection of the HBV DNA. This HBV persistence was abolished by injecting anti-PD-L1 antibody or by the depletion of macrophages, and was dependent on the expression of HBeAg in these mice as well as in their mothers. We further found that the presence or absence of maternal HBeAg dictated how hepatic macrophages of offspring mice were polarized by HBeAg, leading to either viral persistence or viral clearance. Our studies thus delineated the mechanism of HBV persistence after vertical transmission and identified a crticial role of HBeAg in this process. Our results also raise the possibility of targeting macrophages to treat chronic HBV patients.

Results

Non-transgenic mice born to HBV transgenic mother show persistent HBV replication

By using transgenic mice that carried the 1.3mer HBV genomic DNA, we developed a mouse model to study the possible effect of maternal HBV antigens on HBV replication and persistence in offspring mice. Two HBV transgenic mouse lines Tg05 and Tg38, which carried the wild-type HBV genome and the HBx-negative HBV genome, respectively, were used for the studies. These two mouse lines productively replicated HBV DNA in the liver and released mature HBV virions in the blood (Tian et al., 2011). HBV released from transgenic mice could infect chimpanzees (Guidotti et al., 1999), but it could not infect mouse hepatocytes due to the lack of viral receptors. By crossing female hemizygous HBV transgenic mice to male non-transgenic mice of the same genetic background (C57BL/6), we generated HBV-negative mouse pups, which we named TGD mice for transgenic-derived

mice (Figure 1A). The control mice used in our studies were non-transgenic mice born to non-transgenic mother, whether or not the father was HBV transgenic (Figure 1A). The hydrodynamic injection was used to introduce a plasmid that contained the 1.3mer HBV genomic DNA into the liver of nine-week old TGD mice and control mice (Tian et al., 2011). HBsAg and the viral titer in the serum were then measured by ELISA and real-time PCR, respectively, at different time points after injection (Tian et al., 2011). As shown in Figure 1B, both control mice and TGD mice initially produced more than 10^4 IU/ml of HBsAg in the serum. This HBsAg level declined rapidly in control mice and became undetectable three weeks after injection. In contrast, the HBsAg level in TGD mice declined slowly and was still detectable at about 100 IU/ml at 28 weeks after injection, the study endpoint. The level of virion-associated HBV DNA in the serum peaked at 4 days post-infection with more than 10^6 genome copies/ml in control mice and declined rapidly and became undetectable after 4 weeks. In TGD mice, the virion-associated HBV DNA reduced slightly after day 4 but remained more or less at the same level at about 10^6 genome copies/ml up to 28 weeks after injection (Figure 1B). The persistence of HBV in TGD mice was confirmed by immunostaining of the HBV core protein, which could be detected in a significant number of hepatocytes (Figure 1C), often in clusters (Figure S1A), in TGD mice at 3 months after HBV DNA injection. The quantification analysis revealed that nearly 15% of mouse hepatocytes in TGD mice were HBV-positive (Figure S1B). In contrast, the HBV core protein could not be detected in the hepatocytes of control mice at the same time point after injection. Similarly, HBV DNA replicative intermediates (RI) could also be detected by Southern-blot in the TGD mouse liver at 3 months post-injection (Figure 1D). The pattern of the HBV RI DNA in TGD mice was similar to that detected in the liver of Tg38 HBV transgenic mice. No HBV RI DNA could be detected in the liver of control mice three months after HBV DNA injection. We had also analyzed the antibody response. As shown in Figure 1E, the anti-HBsAg antibody could be detected in the serum of control mice, which peaked at 4 weeks after injection, but could not be detected in TGD mice. TGD mice born to Tg05 mice or Tg38 mice generated results with no discernable differences, indicating that HBV persistence in TGD mice was independent of the HBx expression in the mother. Since HBV could not persistently replicate in control mice whether or not the father was HBV transgenic (Figure 1A), these results indicated an important maternal effect on the establishment of HBV persistence in TGD mice.

To determine whether the tolerance of TGD mice to HBV was life-long, we also injected 6–8 month-old TGD mice with the HBV genome. As shown in Figure S1C, 80% of 6–8-month old mice remained HBsAg-positive 3 weeks after DNA injection and this percentage was reduced to 40% after 8 weeks. The analysis of HBV DNA in the serum revealed a similar trend, with 80% of mice remained HBV DNA-positive after 4 weeks, which was reduced to 40% after 8 weeks. These results indicated that TGD mice became less tolerant to HBV as they grew older. We also analyzed whether the tolerance to HBV could be transmitted to the offspring of TGD mice. As shown in Figure S1D, HBV could not establish persistence in the nine-week old offspring of TGD mice, indicating that the tolerance was not established in the germline. These results indicated that HBV established persistent replication more efficiently in younger TGD mice than in older TGD mice, and its ability to establish persistence was limited to TGD mice and not their descendants. As Tg05 and Tg38 mice

generated the same results, we used Tg05 mice for our subsequent studies unless indicated otherwise.

TGD mice injected with HBV DNA have impaired HBV-specific CTL response

To understand why HBV could persist in TGD mice but not in control mice, we analyzed the level of HBV-specific $CD8^+$ T cells in TGD mice and control mice two weeks after the injection of HBV DNA. Mononuclear cells isolated from the liver and the spleen were stimulated with a peptide derived from the HBV core protein (amino acids 93–100, MGLKIRQL) as previously described (Yang et al., 2010). The IFN-γ-producing CD8+ T cells were then analyzed by flow cytometry. As show in Figure 2A, both control mice and TGD mice injected with the pUC19 vector DNA had few activated CD8+ T cells upon stimulation with the HBV peptide. In contrast, for mice injected with HBV DNA, the population of interferon-γ (IFN-γ)-positive $CD8^+$ T cells was 2.8% in the liver of control mice but 0.5% in TGD mice. A similar reduction of IFN-γ-positive $CD8^+$ T cells was also observed in the spleen of TGD mice (0.9%) when compared with the control mice (1.9%). When peptides derived from the HBV X protein (HBx) and the HBV polymerase (pol) were also used to stimulate $CD8^+$ T cells isolated from the mouse liver, the population of IFN-γ-positive $CD8^+$ T cells was also lower in TGD mice than in control mice (Figure S2A). The staining of hepatic $CD8^+$ T cells with the tetramer containing a peptide derived from the HBV core protein revealed a similar reduction of HBV-specific $CD8^+$ T cells in TGD mice when compared with the control mice (Figure 2B and S2B), although such difference was not observed at day 6 after DNA injection, when few of the CD8+ T cells could be stained by the HBV core tetramer (Figure S2C). We had also analyzed the expression levels of Ki67, which is a marker for cell proliferation, in $CD8^+$ T cells that were stained by the HBV core tetramer. As shown in Figure S2D, the population of HBV-specific $CD8^+$ T cells that expressed high levels of Ki67 was reduced in TGD mice when compared with the control mice. We also analyzed granzyme B, which is correlated with the cytolytic functions of $CD8^+$ T cells. Similarly, the expression level of granzyme B in intrahepatic $CD8^+$ T cells was reduced in TGD mice (Figure 2C). These results together indicated that the $CD8^+$ T cell response to HBV was impaired in TGD mice, which was perhaps the reason why HBV was able to persist in these mice. In contrast to $CD8^+$ T cells, the depletion of $CD4^+$ T cells with the anti-CD4 antibody did not abolish the persistence of HBV in TGD mice, although it reduced the ability of control mice to clear HBV (Figure 2D).

To further investigate why the $CD8^+$ T cell response was impaired in TGD mice, we analyzed the expression level of PD-1 in $CD8^+$ T cells, as PD-1 is a negative regulator of $CD8^+$ T cells (Isogawa et al., 2013; Maier et al., 2007). TGD mice and control mice were injected with the HBV genomic DNA and then sacrificed at different time points after DNA injection for the analysis of hepatic mononuclear cells using flow cytometry. As shown in Figure 2E, the percentage of $CD8^+$ T cells that expresses a high level of PD-1 increased in both TGD and control mice after HBV DNA injection. This increase reached a peak at week 3 post-injection and declined thereafter. Importantly, the percentage of $CD8^+$ T cells that expressed a high level of PD-1 was significantly higher in TGD mice than in control mice at every time point after injection. The representative flow cytometry results are shown in Fig. 2F. Similarly, when the HBV core tetramer was used to stain $CD8^+$ T cells, approximately

20% of HBV-specific $CD8^+$ T cells isolated from the control mouse liver expressed a high level of PD-1, but this percentage was increased to nearly 90% when the TGD mice were analyzed (Figure 2B). These results suggested that the impairment of $CD8^+$ CTL response in TGD mice might be due to the increased expression level of PD-1 in those cells.

PD-L1 expression is increased in hepatic macrophages of TGD mice

PD-1 is activated by its ligands PD-L1 and PD-L2. We focused our attention on hepatic macrophages (i.e., Kupffer cells) and PD-L1, as Kupffer cells had previously been shown to express a high level of PD-L1 following adoptive transfer of HBV-specific CTLs into HBV transgenic mice (Maier et al., 2007). As shown in Figure 3A, approximately 4–5% of Kupffer cells in control mice and TGD mice had high expression levels of PD-L1 on day 14 after the injection of the control pUC19 DNA. This percentage increased to ~38% in control mice and ~78% in TGD mice when they were injected with the HBV DNA. Due to the high expression levels of PD-L1 in most of the Kupffer cells in TGD mice, it was conceivable that these macrophages mediated the suppression of CD8+ T cells.

Anti-PD-L1 antibody treatment abolishes HBV persistence in TGD mice

To test whether the interaction between PD-1 and PD-L1 was indeed responsible for HBV persistence in TGD mice, we injected TGD mice with the anti-PD-L1 antibody to disrupt their interaction 2 days before HBV DNA injection and once again at 14 days after DNA injection. The isotype antibody was used as the control. The mouse serum was collected at different time points for up to 8 weeks after HBV DNA injection for the analysis of HBV persistence. As shown in Figure 3B, the injection of the anti-PD-L1 antibody reduced HBsAg and HBV DNA in the serum to an undetectable level after 3 and 4 weeks, respectively. In contrast, the isotype antibody control did not affect the persisence of HBsAg or HBV DNA up to the study endpoint. We also monitored the HBV-specific $CD8^+$ T cells in the liver by flow cytometry at 14 days after HBV DNA injection. As shown in Figure 3C, the control antibody had little effect on HBV-specific $CD8^+$ T cells, which remained low at 0.6% of the hepatic $CD8^+$ T cell population, similar to what was observed in TGD mice without the antibody treatment (see Figure 2A). In contrast, the anti-PD-L1 antibody increased the HBV-specific $CD8^+$ T cells to 2.8%, which is a level similar to what was observed in control mice injected with the HBV DNA (also see Figure 2A). This injection of anti-PD-L1 antibody did not reduce the population of Kupffer cells (Figure 3D). These results indicated that the injection of the anti-PD-L1 antibody, which presumably disrupted the interaction between PD-1 and PD-L1, could restore the $CD8^+$ T cell activity and lead to HBV clearance.

Hepatic macrophages are required for HBV persistence in TGD mice

Our observations that the great majority of Kupffer cells of TGD mice expressed high levels of PD-L1 after HBV DNA injection and the treatment of TGD mice with the anti-PD-L1 antibody led to HBV clearance suggested an important role of these macrophages in HBV persistence. To test this possibility, we injected TGD mcie with clodronate-liposome, which had been shown to deplete Kupffer cells in mice (Sitia et al., 2011; Van Rooijen and Sanders, 1996). As shown in Figure 4A, 7% of hepatic mononuclear cells was $F4/80^+CD11b^+$ (i.e. macrophages) two days after the injection with the PBS-liposome

control, but only 0.4% of them was F4/80$^+$CD11b$^+$ after the injection with clodronate-liposome. This result indicated that clodronate-liposome could deplete Kupffer cells. To further confirm this result, we immunostained the liver tissue sections with the anti-F4/80 antibody. As shown in Figure 4B, while F4/80$^+$ cells could be detected in the liver of mice injected with PBS-liposome, few of them could be identified in the liver of mice injected with clodronate-liposome. These results together indicated that clodronate-liposome could efficiently deplete Kupffer cells.

We next tested whether the depletion of Kupffer cells with clodronate-liposome could affect HBV persistence in TGD mice. TGD mice were treated with clodronate-liposome or the PBS-liposome control once every five days and injected with the HBV DNA two days after the first liposome treatment. As shown in Figure 4C, while PBS-liposome had no effect on the persistence of HBsAg and HBV DNA in TGD mice up to 8 weeks, the study endpoint, clodronate-liposome reduced HBsAg and HBV DNA in TGD mice to an undetectable level after 3 and 4 weeks, respectively. We also analyzed HBV-specific CD8$^+$ T cells in the mouse liver 14 days after HBV DNA injection. As shown in Figure 4D, PBS-liposome had no effect on the level of HBV-specific CD8$^+$ T cells, which remained low at 0.4%. In contrast, clodronate-liposome increased the activated CD8$^+$ T cell level to 3%, a level similar to what was observed in control mice injected with the HBV DNA (Figure 2A) or TGD mice treated with the anti-PD-L1 antibody (Figure 3C). These results confirmed an important role of Kupffer cells in suppressing the HBV-specific CTL response.

HBeAg is required for establishment of HBV persistence

It has been suggested that HBeAg may be important for HBV persistence after vertical transmission (Milich and Liang, 2003; Okada et al., 1976; Ou, 1997). To test this possibility, we engineered an HBV mutant that contained a G to A mutation at nucleotide 1896 (Figure S3A). This mutation, which is frequently found in HBeAg-negative mutant, converted codon 28 of the precore sequence from UGG to the UAG stop codon. A compensatory mutation of C to U at nucleotide 1858 was also created to maintain the stability of the overlapping epsilon structure (Lok et al., 1994). As shown in Figure S3B, these mutations did not affect the expression of HBsAg in Huh7 cells, a human hepatoma cell line, but it abolished the expression of HBeAg. The HBV DNA replication efficiency of this mutant was not reduced but rather, was slightly increased when it was compared with the wild-type virus (Figure S3C), in agreement with the previous report (Lamberts et al., 1993; Scaglioni et al., 1997). We then injected the 1.3mer HBV DNA containing this HBeAg-negative mutation into control and TGD mice. The HBeAg-negative mutant was not able to persist in either control mice or TGD mice (Figure 5A). The HBsAg and DNA became undetectable in the serum of control mice and TGD mice after 3 and 4 weeks, respectively. The analysis of hepatic mononuclear cells revealed that approximately 3% of those cells were HBV-specific CD8$^+$ T cells (Figure S3D), which was similar to what was observed in the control mice injected with the wild-type HBV DNA (see Figure 2A). These results indicated that HBeAg was important for HBV to suppress CD8$^+$ T cell response and establish persistence in TGD mice.

To test whether the expression of HBeAg in the mother was also important for HBV to establish persistent replication in TGD mice, we produced two transgenic mouse lines Tg44

and Tg45 that carried the 1.3mer HBeAg-negative HBV genomic DNA. Tg44 mice had a circulating HBV titer of ~2×10^8 genome copies/ml and Tg45 had a circulating HBV titer of about 3×10^6 genome copies/ml (Figure S3E). HBV RNA transcripts could be detected in the liver of these mouse lines, but, consistent with their circulating HBV titers, the level of replicating HBV DNA was significantly higher in Tg44 mice than in Tg45 mice (Figure S3F). Both mouse lines produced more than 10^4 IU/ml of HBsAg in the serum but no detectable level of HBeAg (Figure S3G). Hemizygous female Tg44 and Tg45 mice were crossed to male non-transgenic mice for the production of HBV-negative mouse pups. These HBeAg-naive TGD mice were then injected with the 1.3mer wild-type HBV DNA at 9 weeks of age. As shown in Figure 5B, the wild-type HBV was not able to persist in either control mice or HBeAg-naive TGD mice and its HBsAg and virion-associated DNA became undetectable after 4 weeks. The use of either Tg44 or Tg45 female mice for breeding generated the same results. These results indicated that, not only was the continuous expression of HBeAg important for HBV to estabilsh persistent replication in TGD mice, but the expression of HBeAg in the mother was also important.

HBeAg differentially effects hepatic macrophage polarization in control versus TGD mice

The observation that Kupffer cells played a critical role in HBV persistence in TGD mice and this persistence required maternal HBeAg prompted us to determine how maternal HBeAg might have affected Kupffer cells. Macrophages may be induced to differentiate into the M1 pro-inflammatory phenotype characterized by the expression of high levels of inducible nitric oxide synthase (iNOS) and pro-inflammatory cytokines, or into the M2 anti-inflammatory phenotype characterized by the expression of anti-inflammatory genes (Murray and Wynn, 2011). To understand how Kupffer cells might have been affected by maternal HBeAg, we isolated Kupffer cells from control mice and TGD mice and analyzed their polarization responses to HBV antigens *ex vivo*. Huh7 cells were transfected with the control vector, the 1.3mer wild-type HBV genomic DNA, the 1.3mer HBeAg-negative HBV genomic DNA, or the expression plasmid for the HBV precore protein, the precursor of HBeAg. The incubation media were harvested two days post-transfection and analyzed for the presence of HBV antigens. As shown in Figure S4A and S4B, the incubation media of cells transfected with the wild-type HBV genomic DNA contained HBsAg, HBeAg and the HBV core particle, those transfected with the HBeAg-negative HBV genome contained HBsAg and the HBV core particle but no HBeAg, and those transfected with the precore protein expression plasmid contained only HBeAg with no HBsAg or the core particle. These incubation media were then used to stimulate Kupffer cells, which were collected 48 hours later with a purity of >90% (Figure S4C) and lysed for the isolation of total RNA for the analysis of expression of M1 and M2 markers by real-time RT-PCR. As shown in Figure 6A, when Kupffer cells isolated from the control mice were analyzed, the incubation media of cells transfected by the wild-type HBV DNA, the mutant HBV DNA and the precore DNA could all induce the expression of iNOS, and cytokines TNF-α and IL-1β, which are markers of M1 polarization. However, when Kupffer cells isolated from TGD mice were analyzed, only the incubation media harvested from cells transfected with the HBV mutant DNA could induce the expression of these three M1 markers. As the only difference between wild-type and mutant HBV was the HBeAg, these results indicated an active role of HBeAg in preventing the M1 polarization of Kupffer cells isolated from TGD mice. We also

analyzed the expression of Arginase-1 (Arg-1), mannose receptor-1 (Mrc-1) and IL-10, which are markers of M2 polarization. As shown in Figure 6B, none of the incubation media could induce the expression of these three markers in Kupffer cells isolated from control mice. However, the incubation media of cells transfected by either the wild-type HBV DNA or the precore DNA, but not those transfected by the mutant HBV DNA, could induce the expression of these three M2 markers in Kupffer cells isolated from the TGD mice. Since the mutant HBV could not express HBeAg, the results shown in Figure 6B indicated that HBeAg was essential and sufficient for the induction of M2-like phenotype of Kupffer cells isolated from TGD mice.

Note that Kupffer cells that underwent M2 polarization also expressed an increased level of PD-L1 (Figure S4D), which is consistent with the results shown in Figure 3A. In addition, Kupffer cells isolated from TGD mice injected with the HBV DNA plasmid also expressed a higher level of IL-10 (Figure 6C), confirming the *ex vivo* results. Taken together, the results shown in Figure 6 indicated that HBeAg had two distinct activities. It promoted the M1-like pro-inflammatory response of Kupffer cells in control mice and promoted the M2-like anti-inflammatory response of Kupffer cells in TGD mice. It also enhanced the expression PD-L1 in Kupffer cells of TGD mice. These activities led to HBV clearance in control mice and HBV persistence in TGD mice.

Discussion

Although HBeAg was first identified in HBV patients more than 40 years ago (Magnius and Espmark, 1972), its biological functions remained enigmatic as it is not required for HBV replication both *in vitro* and *in vivo* but yet it is highly conserved in HBV and its related animal viruses. In this report, by studying TGD mice, we demonstrated that maternal HBeAg could condition hepatic macrophages of the offspring to suppress the CTL response to HBV in the presence of HBeAg, resulting in HBV persistence. This finding demonstrated the importance of HBeAg in HBV persistence after vertical transmission and explains why it is highly conserved among hepadnaviruses. By analyzing the immune responses of TGD mice and control mice to HBV, we found that the ability of HBV to persist in TGD mice was due to an impaired CTL response to HBV, which was associated with the increased expression of PD-1 in $CD8^+$ T cells and PD-L1 in hepatic macrophages. As either the disruption of PD-1 and PD-L1 interaction with the anti-PD-L1 antibody or the depletion of macrophages could lead to the activation of the CTL response and viral clearance, the PD-1 and PD-L1 interaction between $CD8^+$ T cells and hepatic macrophages was most likely responsible for the exhaustion of $CD8^+$ T cells in TGD mice. These findings have important clinical implications, as it indicated that it might be possible to treat chronic HBV patients by disrupting the interaction between PD-1 and PD-L1 using antibodies or by transiently depleting macrophages, since most chronic HBV patients acquired the virus via vertical transmission and their hepatic macrophages are expected to play an important role in suppressing the CTL response, as our results would predict.

It had previously been shown that the HBV genomic DNA inserted in an adeno-associated virus (AAV) vector, when injected into the liver of C57BL/6 mice, could lead to HBV persistence in a fraction of mice, apparently due to a unique feature of the AAV vector and

not due to HBeAg (Lin et al., 2010; Lin et al., 2012). It was subsequently demonstrated that a defect in the HBV core particle assembly could prolong the HBV persistence in that mouse model, which could be abolished by the injection of the anti-PD-1 antibody (Lin et al., 2012; Tzeng et al., 2012). The lack of effect of HBeAg on HBV persistence in that AAV-HBV mouse model was not surprising, as HBV persistence was established via the help of the AAV vector and not due to the effect of the maternal HBeAg. Although this AAV-HBV mouse model is not clinically relevant, its finding that the anti-PD-1 antibody could abolish HBV persistence nevertheless supported the concept that the disruption of the interaction between PD-1 and PD-L1 might be used to facilitate HBV clearance in patients.

For maternal HBeAg to predispose hepatic macrophages of the offspring to suppress the CTL response to HBV, it will require the exposure of the immune system of the offspring mice to maternal HBeAg. It is possible that maternal HBeAg may be able to cross placenta to induce tolerance *in utero* as previously suggested (Milich et al., 1990; Wang and Zhu, 2000), although it should be noted that whether HBeAg can indeed cross the mouse placenta has been disputed (Reifenberg et al., 1998). Alternatively, it is also possible that HBeAg may sensitize macrophages or their progenitor cells during delivery or perinatally such as via colostrum feeding. This latter possibility is supported by the observations that the development of hepatic macrophages is age-dependent (Publicover et al., 2013), and thus the perinatal exposure may still allow HBeAg to predispose hepatic macrophages to suppress immune responses to HBV. Hepatic macrophages are established prior to birth and can maintain themselves during the adulthood (Yona et al., 2013). Our observation that older TGD mice were less tolerant to HBV might be due to the loss of these macrophages as mice grew older. In any case, the conditioning of hepatic macrophages early in life by maternal HBeAg allowed them to display the M2-like anti-inflammatory phenotype and expressed increased levels of PD-L1 when they encounter HBeAg again later in life. Without the conditioning by maternal HBeAg, hepatic macrophages would be induced by HBeAg to display the M1-like pro-inflammatory phenotype, which would favor viral clearance. Although our mouse model is not identical to natural HBV infection in patients after vertical transmission, our studies using this model provided a mechanism to explain how HBV may establish persistent infection in children after vertical transmission and defined the role of HBeAg in this process. Our findings also indicate that targeting macrophages during persistent HBV infection may have therapeutic benefits.

Experimental Procedures

Production of TGD mice and HBeAg-naïve TGD mice

All of the mice used in our studies had the C57BL/6 genetic background. Tg05 and Tg38 were HBV transgenic mouse lines that had been previously described (Tian et al., 2011). Tg44 and Tg45 were two independent mouse lines that carried the 1.3mer HBeAg-negative HBV genomic DNA. They were produced at the USC Trangenic Mouse Core Facility. Female Tg05 or Tg08 mice that carried one allele of the HBV DNA genome were crossed with naïve male C57BL/6 mice to produce TGD mice, which were HBV-negative and identified by genotyping using DNA isolated from tail tissues. The HBeAg-naïve TGD mice were produced from female Tg44 or Tg45 mice using the same procedures. Control mice

used in our studies were HBV-negative mice produced from female non-transgenic mice and male non-transgenic mice or male Tg05 mice that carried one allele of the HBV DNA. Littermates were used for breeding whenever it was appropriate to minimize any possible genetic differences. The HBV DNA used for the production of the transgeni mouse lines and our other studies belongs to genotype A (adw2 subtype). Our mouse studies were conducted in accordance with the *Guide for the Care and Use of Laboratory Animals* of the National Institutes of Health and approved by the Institutional Animal Care and Use Committee of the University of Southern California.

Hydrodynamic injection

The 1.3mer HBV genomic DNA cloned in the pUC19 vector and pCMV-p24, which expresses the HBV major surface antigen, was used for the hydrodynamic injection using our previous procedures (Tian et al., 2011). Briefly, 20 μg HBV DNA in a volume of phosphate-buffered saline (PBS) equivalent to 8% of the body weight of the mouse was injected into nine-week old male mice via the tail vein within 5–8 seconds. Twenty-four hours after the injection, the serum was collected for the analysis of HBsAg and HBV DNA. Mice with matched HBsAg levels were used in the studies.

HBV serological assays by ELISA

HBsAg, HBeAg and the anti-HBsAg antibody were analyzed using the ELISA kit following the manufacturer's instructions (International Immuno-Diagnostics, CA). The mouse serum was diluted 50-fold with PBS, and 100 μl of diluted sample was used for the assay. The assays were conducted in triplicate.

Real-time PCR analysis of HBV titers in the mouse serum

HBV titers in the mouse sera were measured by real-time PCR using our previous procedures (Tian et al., 2011). Briefly, 10 μl mouse serum were digested with DNase I (5 IU) and micrococcal nuclease at 37°C for 30 min to remove free HBV DNA and then treated with 100 μllysis buffer (20 mM Tris-HCl, pH7.5, 20 mM EDTA, 50 mM NaCl, and 0.5% SDS) containing 27 μg proteinase K at 65°C overnight. The virion-associated HBV DNA was isolated by phenol-chloroform extraction and ethanol precipitation. The DNA pellet was dissolved in 10 μl TE buffer. The primers used for real-time PCR analysis of HBV DNA were: forward primer, 1552-CCGTCTGTGCCTTCTCATCTG- 1572; and reverse primer, 1667-AGTCCTCTTATGTAAGACCTT-1646. The TaqMan probe used was 1578-CCGTGTGCACTTCGCTTCACCTCTGC-1603.

Real-time RT-PCR analysis for mRNAs of polarization markers of Kupffer cells

Kupffer cells purified from mouse liver tissues were homogenized in Trizol (Invitrogen) and total RNA was isolated following the manufacturer's protocol. The cDNA synthesis was performed using 1 μg RNA, the random hexamer primer (Roche), and the MMLV Reverse Transcriptase kit (Applied Biosystems). The real-time PCR was performed using the Invitrogen Power SYBR® Green PCR Master Mix and the Applied Biosystems 7500 Fast Real-Time PCR System. PCR reactions were carried out in a total volume of 20 μl. The reaction mixture contained 2× SYBR Mix (12.5 μl) from the kit, the primers (0.4 pmol/μl),

Taq DNA polymerase (4 units), and 1 μl cDNA. The 2× SYBR Mix contained the PCR buffer, Mg^{+2}, dNTP mixture, and SYBR Green®. The thermal cycling condition included an initial denaturation step at 95 °C for 10 minutes and 40 reaction cycles consisting of a denaturation step at 95 °C for 15 seconds and an annealing/elongation step at 60 °C for 60 seconds. Fluorescent measurements were taken at the annealing/elongation step. Each sample was run in duplicates and mean Ct values were used for further calculations.

Southern-blot analysis of HBV DNA

The HBV DNA in core particles was isolated using our previously procedures (Tian et al., 2011). Briefly, 50 mg mouse liver was homogenized in 500 μl lysis buffer (10 mM Tris-HCl, pH 7.5, 1 mM EDTA, 50 mM NaCl, and 0.5% Nonidet P-40) containing 100 μg DNase I and micrococcal nuclease for 30 min at 37°C to remove free DNA. The reaction was stopped by the addition of 50 μl 0.5 M EDTA and 300 μg proteinase K and further incubated at 65°C for 16 hours. The core particle-associated HBV DNA was then isolated by phenol-chloroform extraction and ethanol precipitation. The DNA pellet was rinsed with 70% ethanol and analyzed by Southern blot using the ^{32}P-labeled HBV DNA probe.

Immunohistochemistry staining for HBV core protein

Paraffin-embedded liver tissue sections were treated with 0.01 M sodium citrate and heated in the microwave oven for 10 minutes for epitope retrieval. The tissue sections were then blocked using the goat serum and incubated with the rabbit anti-core antibody (Yeh et al., 1990) and the affinity-purified biotinylated goat anti-rabbit IgG. The staining was then developed using the avidin-conjugated horseradish peroxidase (HRP) with diaminiobenzidine (DAB) as the substrate (Ultra-sensitive ABC Peroxidase Staining Kit, Thermo).

Isolation of mononuclear cells from the mouse liver

The mouse liver was perfused with 30 ml PBS via the hepatic portal vein at room temperature. The liver was excised and liver cells were dispersed in PBS containing 2% fetal bovine serum (FBS) and 0.02% NaN_3 at 4°C through a 40-μm nylon cell strainer (DN Falcon #352340). Cells were centrifuged at 500xg at 4°C for 5 minutes. Liver mononuclear cells were then isolated by centrifugation at 700xg in 25 ml of 33.75% sterile Percoll at 25°C for 7 minutes. Cells were incubated with the 1X Red Blood Cell lysis buffer (Sigma) at room temperature for 4 minutes, and washed three times with PBS containing 2% FBS and 0.02% NaN_3 at 4°C with centrifugation at 500xg for 5 minutes after each wash. After the first wash, cells were again filtered through a 40-μm nylon cell strainer and, after the last wash, cells were resuspended in 1 ml PBS containing 2% FBS and 0.02% NaN_3 and counted.

Flow cytometry

The following antibodies, which were all purchased from eBioscience, San Diego, were used for flow cytometry: anti-mouse CD3 eFluor 450 (cat. 48-0032), anti-mouse CD4 APC-eFluor 780 (cat. 47-0042), anti-mouse CD8 APC (cat. 11-0081), anti-mouse F4/80 PE-Cy7 (cat. 25-4801), anti-mouse CD11b APC-Cy7, anti-mouse-IFN-γ PE (cat. 12-7311), anti-

mouse PD-1 PE (12-9985), anti-mouse PD-L1 PE (cat. 12-5982), anti-mouse IL-10 (cat. 11-7101) and anti-mouse Ki67 eFluor 450 (cat. 48-5698). Two million cells per sample were used for flow cytometry. Cells were incubated with Fc Block for 15 minutes at 4°C in darkness to block the FcγR and then stained with fluorochrome-conjugated antibodies for 30 minutes at 4°C also in darkness. Cells were then analyzed using a Canto II (BD Bioscience, CA) 8-color flow cytometer, and data were analyzed using FlowJo software (Tree Star, Inc., Ashland, OR).

Intracellular Staining

Cells were fixed in 100 μl fixation/permeabilization buffer (eBioscience, Cat: 00-5123-43) and incubated in darkness at room temperature for 20 minutes. 0.5 ml of 1× permeabilization buffer (eBioscience, Cat: 00-8333-56) was then added to each tube and cells were centrifuged at 500×*g* at room temperature for 5 minutes. After the removal of the supernatant, cells were washed twice with 0.5 mL 1× permeabilization buffer, resuspended in 100 μl 1× permeabilization buffer, and stained with fluorochrome-labeled antibodies at room temperature for 60 minutes in darkness for the detection of intracellular antigens. Cells were finally washed twice with PBS containing 2% FBS and 0.02% NaN_3, resuspended in the same buffer and analyzed using a flow cytometer.

Analysis of activated $CD8^+$ T cells

Mononuclear cells (2×10^6) isolated from the mouse liver or spleen were seeded in U-bottom plates and treated with brefeldin A (cat. 00-4506-51, eBioscience), CD28 (0.5 μg/ml) (cat. 16-0281-82, eBioscience), and K^b-restricted HBV core-derived $CD8^+$ epitope (core 93–100: MGLKIRQL); HBV X-derived $CD8^+$ epitope (HBX 92-100:VLHKPTLGL); HBV polymerase-derived $CD8^+$ epitope (polymerase 377-386: LVVDFSQFSR) or the control peptide (DAPIYTNV). After stimulation with the peptides, cells were harvested, washed with PBS containing 2% FBS, and resuspended in the same wash buffer. The staining of HBV core tetramer (MBL, cat. TS-M537-1) was performed according to the manufacturer's instructions. The staining of IFN-γ and the cell surface marker CD8 was performed as described above.

Depletion of hepatic macrophages and CD4 T cells

Mice were injected via the tail vein with 200 μl of clodronate-liposome (5 mg/ml) or PBS-liposome suspension once every five days (ClodronateLiposome.com, Netherlands). The depletion of hepatic macrophages was analyzed by FACS and immunofluorescence staining. For the depletion of CD4 T cells, mice were intraperitoneally injected with 100 μg anti-mouse CD4 antibody (Biolegend, cat:100435) at day 0, 1, 2, 5, 8, 14, 17 and 20 after HBV DNA injection using published procedures (Ebert et al., 2015).

Isolation of hepatic macrophages from mice

The mouse liver was digested *in situ* with pronase and collagenase by sequential perfusion, and non-parenchymal liver cells were fractionated on a discontinuous arabinogalactan gradient by ultracentrifugation. The fraction enriched for hepatic macrophages was further purified by the adherence method.

Statistical analyses

Data were presented as the mean ± s.e.m., and *p* values were determined by two-tailed Student's *t*-test using GraphPad Prism software. Differences that were statistically significant were indicated by asterisks in the figures.

Supplementary Material

Refer to Web version on PubMed Central for supplementary material.

Acknowledgments

We wish to thank Dr. Frank Chisari for critical reading of this manuscript and for providing valuable comments. We also would like to thank the Non-parenchymal Liver Cell Core Facility of the USC Research Center for Alcoholic Liver and Pancreatic Diseases for help with the isolation of hepatic macrophages. This work was supported by NIH grants DK100257 and CA177337.

References

Carman WF, Jacyna MR, Hadziyannis S, Karayiannis P, McGarvey MJ, Makris A, Thomas HC. Mutation preventing formation of hepatitis B e antigen in patients with chronic hepatitis B infection. Lancet. 1989; 2:588–591. [PubMed: 2570285]

Chisari FV, Isogawa M, Wieland SF. Pathogenesis of hepatitis B virus infection. Pathologie-biologie. 2010; 58:258–266. [PubMed: 20116937]

Ebert G, Preston S, Allison C, Cooney J, Toe JG, Stutz MD, Ojaimi S, Scott HW, Baschuk N, Nachbur U, et al. Cellular inhibitor of apoptosis proteins prevent clearance of hepatitis B virus. Proceedings of the National Academy of Sciences of the United States of America. 2015; 112:5797–5802. [PubMed: 25902529]

Guidotti LG, Rochford R, Chung J, Shapiro M, Purcell R, Chisari FV. Viral clearance without destruction of infected cells during acute HBV infection. Science. 1999; 284:825–829. [PubMed: 10221919]

Isogawa M, Chung J, Murata Y, Kakimi K, Chisari FV. CD40 activation rescues antiviral CD8(+) T cells from PD-1-mediated exhaustion. PLoS pathogens. 2013; 9:e1003490. [PubMed: 23853599]

Keir ME, Butte MJ, Freeman GJ, Sharpe AH. PD-1 and its ligands in tolerance and immunity. Annu Rev Immunol. 2008; 26:677–704. [PubMed: 18173375]

Lamberts C, Nassal M, Velhagen I, Zentgraf H, Schroder CH. Precore-mediated inhibition of hepatitis B virus progeny DNA synthesis. Journal of virology. 1993; 67:3756–3762. [PubMed: 8510204]

Lin YJ, Huang LR, Yang HC, Tzeng HT, Hsu PN, Wu HL, Chen PJ, Chen DS. Hepatitis B virus core antigen determines viral persistence in a C57BL/6 mouse model. Proceedings of the National Academy of Sciences of the United States of America. 2010; 107:9340–9345. [PubMed: 20439715]

Lin YJ, Wu HL, Chen DS, Chen PJ. Hepatitis B virus nucleocapsid but not free core antigen controls viral clearance in mice. Journal of virology. 2012; 86:9266–9273. [PubMed: 22718814]

Liu CJ, Chen PJ, Lai MY, Kao JH, Chen DS. Evolution of precore/core promoter mutations in hepatitis B carriers with hepatitis B e antigen seroreversion. J Med Virol. 2004; 74:237–245. [PubMed: 15332272]

Lok AS, Akarca U, Greene S. Mutations in the pre-core region of hepatitis B virus serve to enhance the stability of the secondary structure of the pre-genome encapsidation signal. Proceedings of the National Academy of Sciences of the United States of America. 1994; 91:4077–4081. [PubMed: 8171038]

Magnius LO, Espmark JA. New specificities in Australia antigen positive sera distinct from the Le Bouvier determinants. Journal of immunology. 1972; 109:1017–1021.

Maier H, Isogawa M, Freeman GJ, Chisari FV. PD-1:PD-L1 interactions contribute to the functional suppression of virus-specific CD8+ T lymphocytes in the liver. J Immunol. 2007; 178:2714–2720. [PubMed: 17312113]

Maini MK, Schurich A. The molecular basis of the failed immune response in chronic HBV: therapeutic implications. Journal of hepatology. 2010; 52:616–619. [PubMed: 20185199]

Milich D, Liang TJ. Exploring the biological basis of hepatitis B e antigen in hepatitis B virus infection. Hepatology. 2003; 38:1075–1086. [PubMed: 14578844]

Milich DR, Jones JE, Hughes JL, Price J, Raney AK, McLachlan A. Is a function of the secreted hepatitis B e antigen to induce immunologic tolerance in utero? Proceedings of the National Academy of Sciences of the United States of America. 1990; 87:6599–6603. [PubMed: 2395863]

Murray PJ, Wynn TA. Protective and pathogenic functions of macrophage subsets. Nature reviews Immunology. 2011; 11:723–737.

Okada K, Kamiyama I, Inomata M, Imai M, Miyakawa Y. e antigen and anti-e in the serum of asymptomatic carrier mothers as indicators of positive and negative transmission of hepatitis B virus to their infants. The New England journal of medicine. 1976; 294:746–749. [PubMed: 943694]

Okazaki T, Honjo T. The PD-1-PD-L pathway in immunological tolerance. Trends Immunol. 2006; 27:195–201. [PubMed: 16500147]

Ou JH. Molecular biology of hepatitis B virus e antigen. Journal of gastroenterology and hepatology. 1997; 12:S178–187. [PubMed: 9407336]

Ou JH, Laub O, Rutter WJ. Hepatitis B virus gene function: the precore region targets the core antigen to cellular membranes and causes the secretion of the e antigen. Proceedings of the National Academy of Sciences of the United States of America. 1986; 83:1578–1582. [PubMed: 3006057]

Publicover J, Gaggar A, Nishimura S, Van Horn CM, Goodsell A, Muench MO, Reinhardt RL, van Rooijen N, Wakil AE, Peters M, et al. Age- dependent hepatic lymphoid organization directs successful immunity to hepatitis B. The Journal of clinical investigation. 2013; 123:3728–3739. [PubMed: 23925290]

Publicover J, Goodsell A, Nishimura S, Vilarinho S, Wang ZE, Avanesyan L, Spolski R, Leonard WJ, Cooper S, Baron JL. IL-21 is pivotal in determining age-dependent effectiveness of immune responses in a mouse model of human hepatitis B. The Journal of clinical investigation. 2011; 121:1154–1162. [PubMed: 21393863]

Reifenberg K, Deutschle T, Wild J, Hanano R, Gastrock-Balitsch I, Schirmbeck R, Schlicht HJ. The hepatitis B virus e antigen cannot pass the murine placenta efficiently and does not induce CTL immune tolerance in H-2b mice in utero. Virology. 1998; 243:45–53. [PubMed: 9527914]

Scaglioni PP, Melegari M, Wands JR. Biologic properties of hepatitis B viral genomes with mutations in the precore promoter and precore open reading frame. Virology. 1997; 233:374–381. [PubMed: 9217060]

Sitia G, Iannacone M, Aiolfi R, Isogawa M, van Rooijen N, Scozzesi C, Bianchi ME, von Andrian UH, Chisari FV, Guidotti LG. Kupffer cells hasten resolution of liver immunopathology in mouse models of viral hepatitis. PLoS pathogens. 2011; 7:e1002061. [PubMed: 21655107]

Tian Y, Chen WL, Ou JH. Effects of interferon-alpha/beta on HBV replication determined by viral load. PLoS pathogens. 2011; 7:e1002159. [PubMed: 21829354]

Tzeng HT, Tsai HF, Liao HJ, Lin YJ, Chen L, Chen PJ, Hsu PN. PD-1 blockage reverses immune dysfunction and hepatitis B viral persistence in a mouse animal model. PLoS One. 2012; 7:e39179. [PubMed: 22761734]

Van Rooijen N, Sanders A. Kupffer cell depletion by liposome-delivered drugs: comparative activity of intracellular clodronate, propamidine, and ethylenediaminetetraacetic acid. Hepatology. 1996; 23:1239–1243. [PubMed: 8621159]

Wang JS, Zhu QR. Infection of the fetus with hepatitis B e antigen via the placenta. Lancet. 2000; 355:989. [PubMed: 10768442]

Yang PL, Althage A, Chung J, Chisari FV. Hydrodynamic injection of viral DNA: a mouse model of acute hepatitis B virus infection. Proceedings of the National Academy of Sciences of the United States of America. 2002; 99:13825–13830. [PubMed: 12374864]

Yang PL, Althage A, Chung J, Maier H, Wieland S, Isogawa M, Chisari FV. Immune effectors required for hepatitis B virus clearance. Proceedings of the National Academy of Sciences of the United States of America. 2010; 107:798–802. [PubMed: 20080755]

Yeh CT, Liaw YF, Ou JH. The arginine-rich domain of hepatitis B virus precore and core proteins contains a signal for nuclear transport. Journal of virology. 1990; 64:6141–6147. [PubMed: 2243390]

Yona S, Kim KW, Wolf Y, Mildner A, Varol D, Breker M, Strauss-Ayali D, Viukov S, Guilliams M, Misharin A, et al. Fate mapping reveals origins and dynamics of monocytes and tissue macrophages under homeostasis. Immunity. 2013; 38:79–91. [PubMed: 23273845]

Highlights

- Developed a mouse model to study effect of maternal HBV on persistence in offspring.
- The CTL response to HBV is impaired in the offspring of HBV-positive mothers.
- Depletion of macrophages in offspring restores the CTL response for HBV clearance.
- Maternal HBeAg enhances PD-L1 expression in macrophages of offspring to suppress CTLs.

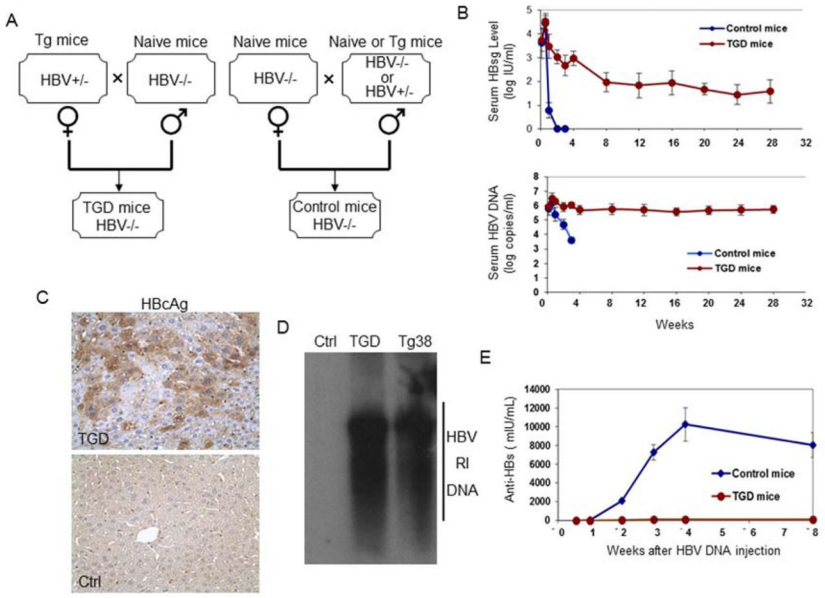

Figure 1. HBV persists in TGD mice but not in control mice

(A) Procedures for the generation of TGD mice and control mice. HBV+/− mice were hemizygous Tg05 or Tg38 HBV transgenic mice. (B) Analysis of HBV persistence in control and TGD mice. The sera of 12 control mice and 13 TGD mice injected with 20 μg 1.3mer HBV DNA were collected at the time points indicated and analyzed for HBsAg by ELISA (upper panel) and HBV DNA by real-time PCR (lower panel). (C) Immunostaining of HBV core protein in the liver of TGD mice (upper panel) and control mice (lower panel). (D) Southern-blot analysis of HBV replicative intermediate (RI) DNA in the mouse liver. The liver tissues of control (Ctrl) and TGD mice were isolated at three months after HBV DNA injection for the analysis. The liver tissue of a 3-month old Tg38 mouse was also analyzed to serve as the control. (E) Analysis of anti-HBsAg antibodies in mouse sera by ELISA. See also Figure S1.

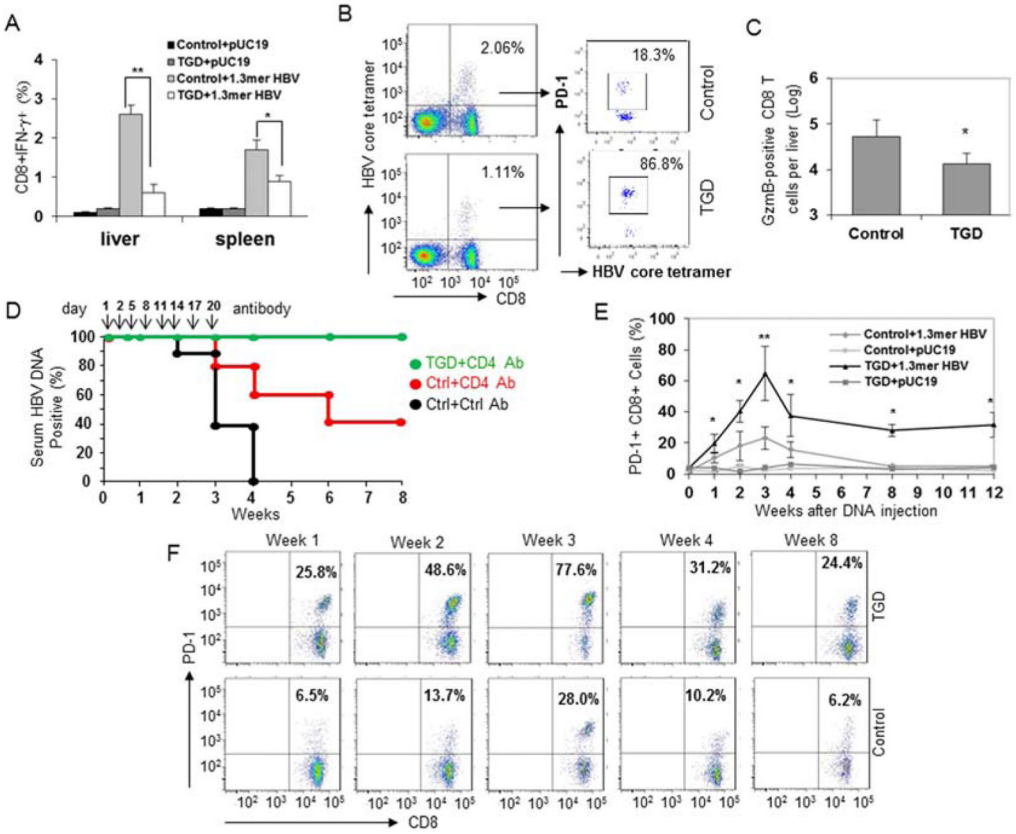

Figure 2. CTL responses to HBV are impaired in TGD mice

(A) Analysis of HBV-specific $CD8^+$ T cells. Control mice and TGD mice injected with pUC19 or HBV DNA were sacrificed at 14 days after injection for the isolation of liver mononuclear cells and spleen cells. These cells were then stimulated with the HBV core peptide (a.a. 93-100) and analyzed by flow cytometry for $CD8^+IFN\text{-}\gamma^+$ cells. The results represent the mean values of at least three mice. (B) $CD8^+$ T cells isolated from the liver of control mice and TGD mice were stained with the HBV core tetramer at 14 days after HBV DNA injection and further analyzed for the expression of PD-1 by flow cytometry. (C) Granzyme B $(GzmB)^+CD8^+$ T cells per mouse liver were quantified by flow cytometry two weeks after HBV DNA plasmid injection. Five mice in each group were analyzed. *, $p<0.05$. (D) Control (Ctrl) and TGD mice were injected with the HBV genomic DNA and treated with the anti-CD4 antibody or the control antibody at the time points indicated. Serum HBV DNA was then analyzed at the time points indicated. Ten mice were analyzed for each group. (E) TGD mice or control mice were injected with the HBV DNA or the control vector pUC19 and sacrificed at different time points for the isolation of intrahepatic lymphocytes, which were analyzed by flow cytometry for the expression of PD-1 and CD8. The results represent the mean values of four different mice. Asterisks mark the data points that were statistically significant when the results between TGD mice and control mice that were injected with the HBV DNA were compared. *, $p<0.05$; **, $p<0.01$. (C) The representative flow cytometry results of $PD\text{-}1^+CD8^+$ cells in TGD mice and control mice at different time points after the injection with the HBV DNA. See also Figure S2.

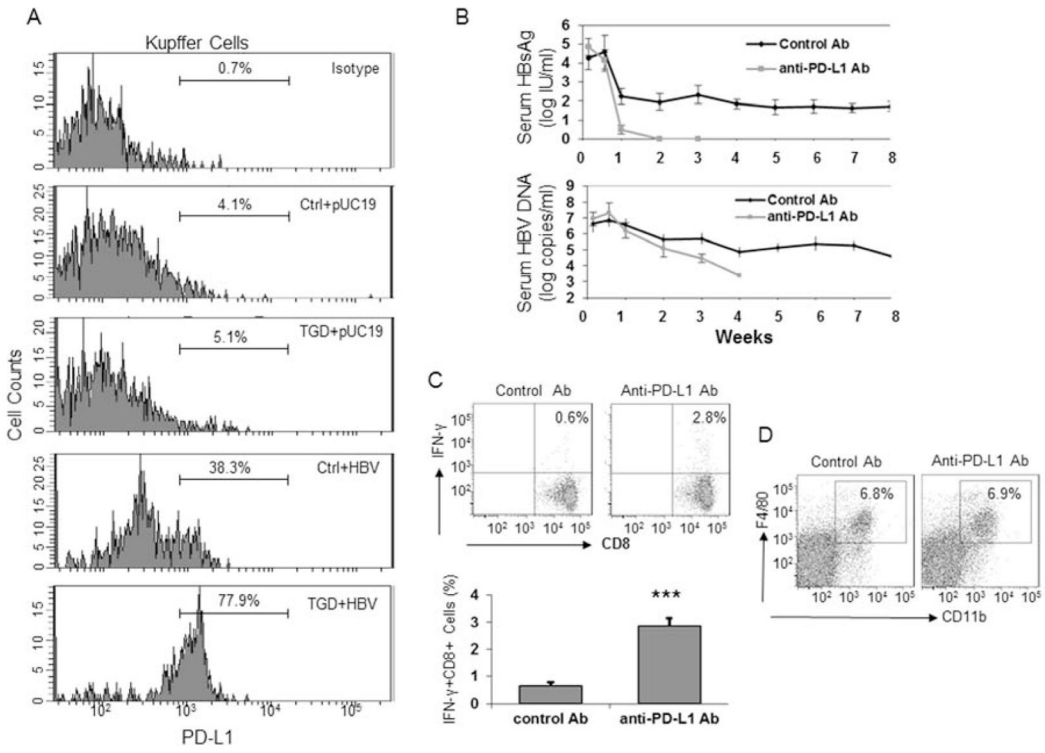

Figure 3. Enhanced expression of PD-L1 in Kupffer cells is critical for HBV persistence in TGD mice

(A) Analysis of PD-L1 expression in Kupffer cells isolated from control (Ctrl) and TGD mice that were injected with pU19 or HBV DNA. The isotype antibody was used as the negative control to stain Kupffer cells isolated from control mice that were injected with pUC19. (B) Analysis of the effect of the anti-PD-L1 antibody on HBV persistence in TGD mice. TGD mice were treated with either the control antibody or the anti-PD-L1 antibody. The serum samples were collected at the time points indicated for HBsAg (upper panel) and HBV DNA (lower panel) analysis. Three different animals were used for each group and the results represented the mean. (C) Analysis of HBV-specific CD8+ T cells. TGD mice treated with either the control antibody or the anti-PD-L1 antibody were analyzed by flow cytometry using the procedures described in the Figure 2 legend. Representative flow cytometry results are show on the top. The results shown in the histogram represent the mean of five different mice in each group. ***, $p<0.005$. (D) Analysis of the effect of the anti-PD-L1 antibody on Kupffer cells. Kupffer cells were isolated from TGD mice two days after the injection of the control antibody or the anti-PD-L1 antibody and analyzed by flow cytometry.

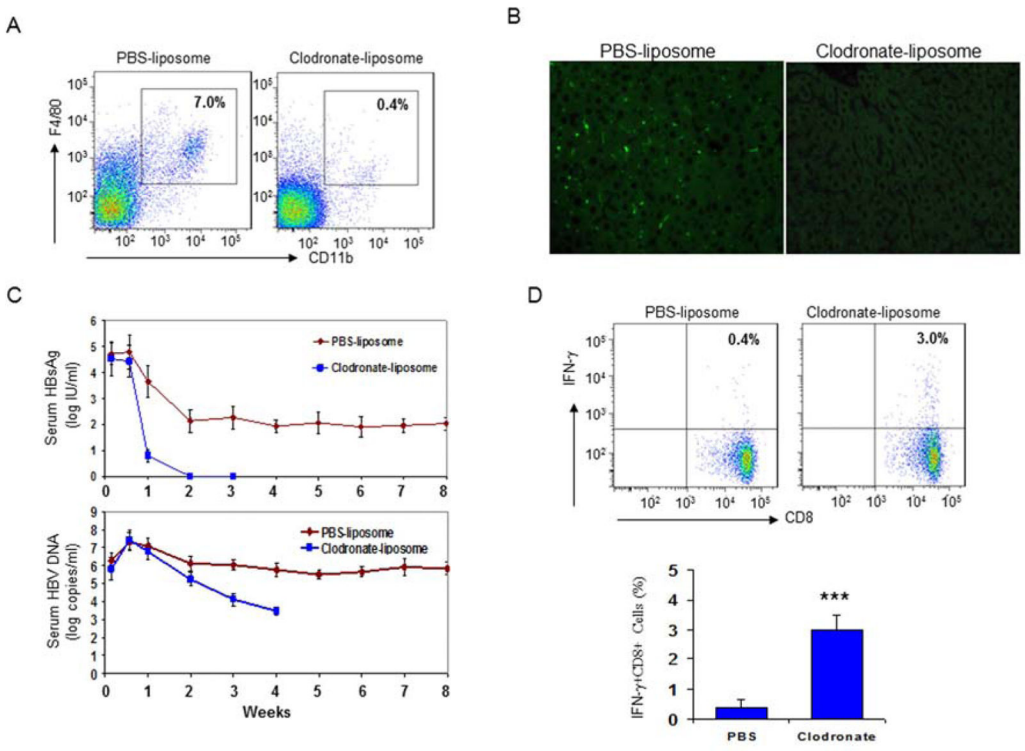

Figure 4. Hepatic macrophages mediate HBV persistence in TGD mice

(A–B) TGD mice were injected with PBS-liposome or clodronate-liposome and sacrificed 48 hours later. Kupffer cells were then analyzed by flow cytometry (A) or immunofluorescence staining using the antibody directed against its cell surface marker F4/80 (B). (C) TGD mice injected with the HBV DNA were treated with PBS-liposome or clodronate-liposome. The sera were collected at the time points indicated for the analysis of HBsAg (upper panel) and HBV DNA (lower panel). The results represent the mean of three different mice. (D) HBV-specific CD8+ T cells were analyzed by flow cytometry as described in the Figure 2 legend. The results shown in the histogram represent the mean values of five different mice. ***, $p<0.005$.

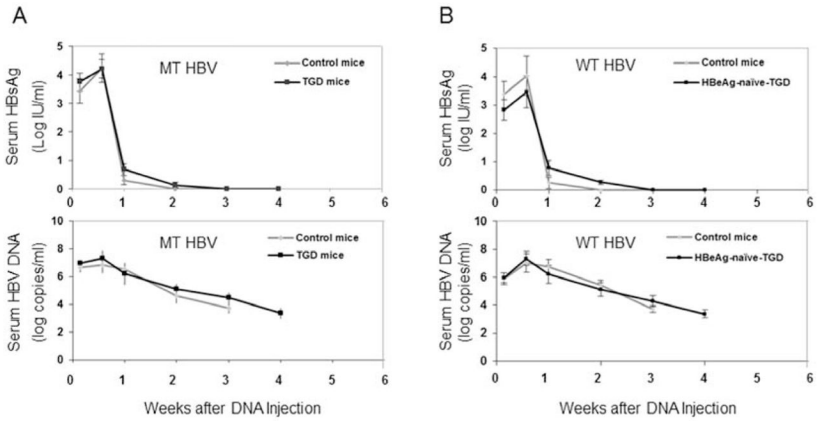

Figure 5. HBeAg is essential for HBV persistence in TGD mice

(A) 12 control mice and 11 TGD mice were injected with the HBeAg-negative HBV DNA (i.e., MT HBV DNA). (B) 12 control mice and 7 HBeAg-naïve TGD mice were injected with the wild-type HBV genomic DNA (i.e., WT HBV DNA). The sera were collected at the time points indicated and analyzed for HBsAg (upper panels) and HBV DNA (lower panels). The results represent the mean. See also Figure S3.

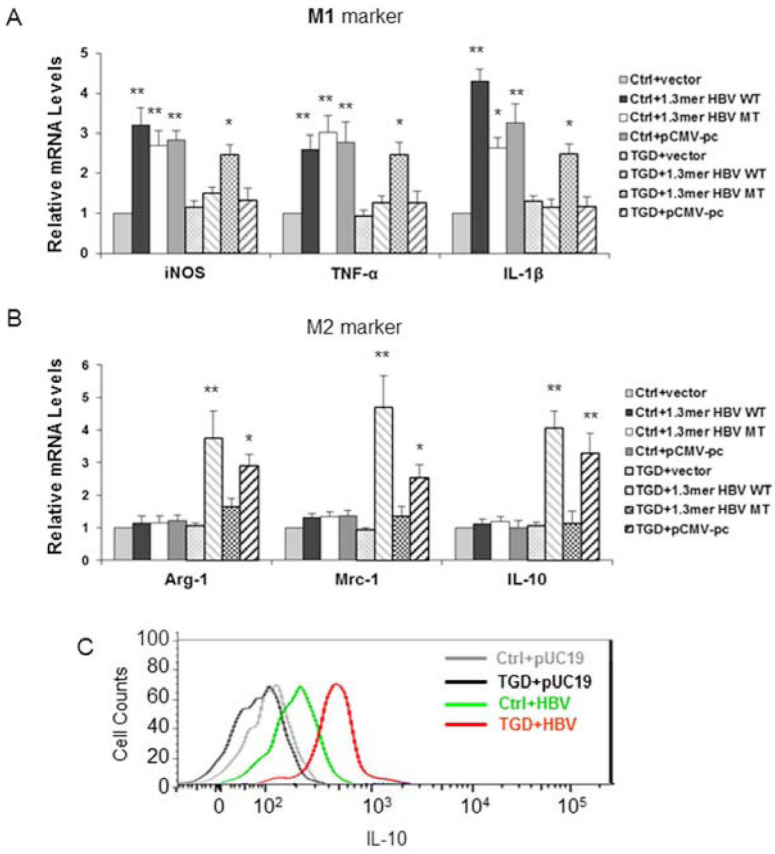

Figure 6. HBeAg differentially effects the polarization of hepatic macrophages of control versus TGD mice

(A–B) Hepatic macrophages were isolated from control mice and TGD mice and treated with the incubation media harvested from Huh7 cells transfected by pUC19, the wild-type HBV DNA, the HBeAg-negative HBV DNA or the HBeAg expression plasmid for 48 hours. Total cellular RNA was then isolated for real-time RT-PCR analysis of the RNA of M1 (A) and M2 (B) markers. Asterisks indicate that the results were statistically significant when they were compared against the vector control. *, $p<0.05$; **, $p<0.01$. (C) Flow cytometry analysis of IL-10 expression in hepatic macrophages isolated from control mice and TGD mice that had been injected with pUC19 or the HBV genomic DNA for two weeks. See also Figure S4.